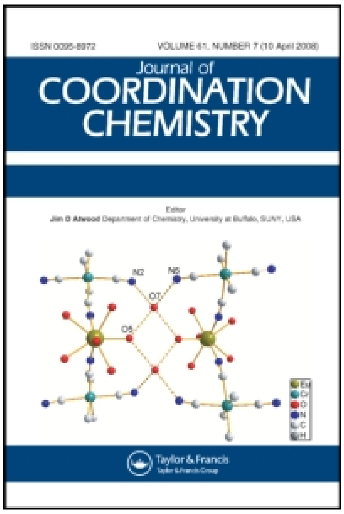

Journal of Coordination Chemistry
Publication details, including instructions for authors and subscription information:
http://www.informaworld.com/smpp/title~content=t713455674

Chloro and azido bonded manganese complexes: synthesis, structural, and magnetic studies

Pooja Tyagi[a]; Udai P. Singh[a]
[a] Department of Chemistry, Indian Institute of Technology, Roorkee, India

To cite this Article Tyagi, Pooja and Singh, Udai P.(2009) 'Chloro and azido bonded manganese complexes: synthesis, structural, and magnetic studies', Journal of Coordination Chemistry, 62: 10, 1613 — 1622
To link to this Article: DOI: 10.1080/00958970802680682
URL: http://dx.doi.org/10.1080/00958970802680682

Journal of Coordination Chemistry
Vol. 62, No. 10, 20 May 2009, 1613–1622

Taylor & Francis
Taylor & Francis Group

Chloro and azido bonded manganese complexes: synthesis, structural, and magnetic studies

POOJA TYAGI and UDAI P. SINGH*

Department of Chemistry, Indian Institute of Technology, Roorkee, India

(*Received 6 April 2008; revised 20 August 2008; in final form 22 August 2008*)

Two manganese complexes, $[Mn_2(tptz)_2Cl_4]\cdot CH_3CN$ (**1**) and $[Mn(tptz(ac)(N_3)(H_2O)]\cdot H_2O$ (**2**) (where tptz = 2,4,6-tri(2-pyridyl)-1,3,5-triazine, ac = acetate anion), were synthesized and characterized by elemental analyses, infrared spectra, and UV–Vis absorption spectral analyses. The structures of both the complexes were determined by single crystal X-ray diffraction analysis. Complex **1** is binuclear with chloro-bridged manganese ions at the Mn–Mn separation of 3.777(27) Å. Each manganese center in **1** is six coordinate with three nitrogens from a tridentate tptz, three chlorides (one terminal and two bridging), adopting a centrosymmetric distorted octahedral geometry. Various hydrogen bonds form 2-D spiral structures in **1** with Mn–Mn separation of 7.421(2) Å along *a*-axis and 9.121(2) Å along *b*-axis. Complex **2** is seven coordinate with pentagonal bipyramidal geometry. The metal center coordinates to three nitrogens from tptz, two oxygens from acetate, one nitrogen from azide, and one oxygen from water. It has a 1-D layered structure, where three independent molecules are linked by uncoordinated water present in the lattice. Magnetic susceptibility in the temperature range 5–300 K for **1** shows the presence of antiferromagnetic interaction between the local high-spin manganese(II) ions with $J = -0.17\,cm^{-1}$.

Keywords: Manganese complexes; Azido; Molecular structure; Magnetic properties

1. Introduction

Preparation and magnetic properties of inorganic polymers with paramagnetic metal ions are important in molecular magnetism [1–3]. Pseudohalide ligands such as azide (N_3^-) have been exploited to bridge paramagnetic moieties into dimers, clusters and polymers [4], serving as a versatile bridging ligand in either end-to-end (EE) or end-on (EO) fashion.

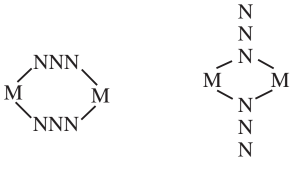

end-to-end end-on

---

*Corresponding author. Email: udaipfcy@iitr.ernet.in

Journal of Coordination Chemistry
ISSN 0095-8972 print/ISSN 1029-0389 online
DOI: 10.1080/00958970802680682

Azide can also coordinate terminally. Terminal azide complexes especially of chromium, manganese and iron play important roles in the preparation of nitride [5]. There are few structurally characterized complexes of Mn II/III with an azide bridge [6–9]. Terminal manganese azide compounds are also very few. Zhang *et al.* [10] reported Mn–azide complexes with nitronyl–nitroxide as precursors in designing molecular-based magnets and crystal structures of the Cu(II) and Mn(II) complexes. Liu *et al.* [11] reported synthesis of transition metal complexes with azide and 3,4-di(2′-pyridyl)-1,2,5-oxadiazle where azide is coordinated terminally. Mantel *et al.* [12] prepared mononuclear six-coordinate azide Mn(III) compounds with tridentate N donor ligands. Ghosh *et al.* [13] synthesized Mn(II) complexes consisting of neutral linear 1-D chains built up by $Mn(N_3)_{-2}$ units connected by two bridging bpds (= 4,4′-bipyridyl disulfide) and of uncoordinated lattice bpds. Examples of seven-coordinate azide manganese complexes are not available in the literature.

The paucity of terminal azide bonded mononuclear manganese compounds prompted us to prepare manganese complexes with tptz ligand. Here, we describe the synthesis and crystal structures of two new manganese(II) complexes with chloride/azide and tptz. To the best of our knowledge, this is the first example of seven-coordinate azide bonded mononuclear manganese(II).

2. Experimental

2.1. *Materials*

All manipulations were performed in aerobic atmosphere. The required solvents were pre-dried from appropriate drying agents by literature methods [14]. 2,4,6-Tri (2-pyridyl)-1,3,5-triazine (tptz) was purchased from Aldrich, Germany and $MnCl_2 \cdot 4H_2O$ (reagent grade) from E. Merck. Other reagents were of the highest grade commercially available and used without purification.

2.2. *Synthesis of complexes*

2.2.1. Synthesis of $[Mn_2(tptz)_2Cl_4] \cdot CH_3CN$ (1). To the hot acetonitrile solution (20 mL) of 2,4,6-tri(2-pyridyl)-1,3,5-triazine (0.20 g, 0.64 mmol) was added $MnCl_2 \cdot 4H_2O$ (0.12 g, 0.64 mmol) and stirred for 1 h. The resultant solution was filtered and yellow crystals suitable for X-ray data collection were obtained from slow evaporation of solvent at room temperature. Yield 69.37% (0.39 g, 0.44 mmol). The complex was analyzed after completely drying under vacuum for several hours. Anal. Calcd (%) for $C_{36}H_{24}N_{12}Cl_4Mn_2$ (876.32): C, 49.34; H, 2.76; N, 19.18. Found: C, 49.60; H, 2.69; N, 19.26. IR(KBr, cm^{-1}): ν(C=N) 1627, ν(C=C) 1568. UV–Vis λ_{max} nm (ε $M^{-1}\,cm^{-1}$) in methanol: 205 (33, 162), 249 (25, 859), 287 (41, 513). Magnetic moment μ_{eff} (300 K) = 5.82 BM/Mn^{2+}.

2.2.2. Synthesis of $[Mn(tptz)(ac)(N_3)(H_2O)] \cdot H_2O$ (2). To the methanolic solution (20 mL) of **1** (0.44 g, 0.50 mmol) was added sodium acetate (0.03 g, 0.50 mmol) and stirred for 30 min. To this solution, 3.0 mL aqueous solution of sodium azide (0.04 g, 0.50 mmol) was added and the reaction mixture further stirred for 30 min. The resulting mixture was filtered and yellow crystals suitable for X-ray data collection were obtained at room temperature in 65.47% (0.16 g, 0.32 mmol) yield. The complex was analyzed after completely drying the sample under vacuum for several hours. Anal. Calcd (%) for $C_{20}H_{17}N_9O_3Mn$ (486.34): C, 49.39; H, 3.52; N, 25.92. Found: C, 49.51; H, 3.66; N, 26.16. IR(KBr, cm^{-1}): $\nu(N_3)$ 2061, ν(C=N) 1638, ν(C=C) 1550, ν_{as}(COO) 1550, ν_s(COO) 1431. UV–Vis λ_{max} nm (ε $M^{-1}\,cm^{-1}$) in methanol: 205 (15, 463), 251 (10, 704), 290 (20, 001). Magnetic moment μ_{eff} (300 K) = 5.83 BM.

2.3. *Physical measurements*

Elemental analyses (C, H, and N) were performed on a Vario EL elementar analyzer. Infrared spectra were obtained on a Thermo Nikolet Nexus spectrometer in KBr. The UV–Vis spectra were recorded on a Perkin–Elmer Lambda 35 UV–Vis spectrophotometer. Cyclic voltammetry was performed using an EG&G potentiostat/galvanostat model 273A on acetonitrile solution of samples containing 0.10 M $[N(n\text{-Bu})_4]PF_6$ as supporting electrolyte. Ferrocene was used as an internal standard and the reported potentials are referenced *versus* the Fc^+/Fc couple. Room temperature magnetic susceptibility measurements were done on a Princeton Applied Research vibrating sample magnetometer Model 155. The variable temperature magnetic susceptibility measurements (2.0–300 K) were performed on a Quantum Design SQUID Magnetometer Model MPMS. Single crystals suitable for X-ray data collection were mounted on a cryoloop using fomblin (mounting glue) and the data were collected on a Bruker Kappa Apex-CCD diffractometer using graphite monochromated Mo-Kα radiation ($\lambda = 0.71073$) at 100 K. The structures were solved by direct methods with anisotropic approximation refinement using the SHELXTL package [15, 16]. Hydrogen atoms were placed in geometrically calculated positions and refined using a riding model. A summary of crystallographic data and refinement parameters for **1** and **2** are given in table 1.

Table 1. Crystallographic data for **1** and **2**.

Complex	**1**	**2**
Formula	$C_{40}H_{30}Cl_4Mn_2N_{14}$	$C_{20}H_{19}MnN_9O_4$
Molecular weight	958.46	504.38
Temperature	100(2) K	100(2) K
Wavelength	0.71073 Å	0.71073 Å
Radiation	Mo-Kα	Mo-Kα
Crystal system	Triclinic	Triclinic
Space group	$P\bar{1}$	$P\bar{1}$
Unit dimensions (Å, °)		
a	7.4208(12)	8.8199(3)
b	9.1209(14)	10.5924(4)
c	14.544(2)	13.0065(4)
α	83.912(10)	98.446(2)
β	78.572(12)	103.358(2)
γ	84.908(10)	110.175(2)
V (Å^3)	957.1(3)	1075.02(7)
Z	1	2
Density (D_x) Mgm^{-3}	1.663	1.558
Diffractometer used	Bruker Kappa Apex	Bruker Kappa Apex
θ range (°)	1.43–28.12	1.66–34.51
Goodness-of-fit on F^2	1.410	0.922
Final R indices [$I > 2\sigma(I)$]	$R_1 = 0.1028$	$R_1 = 0.0454$

3. Results and discussion

3.1. *Electronic spectrum*

The UV–Vis spectra of **1** and **2** in methanol were recorded from 200 to 800 nm displaying intense bands in the range of 205–226, 234–251 and 281–295 nm. The bands at 205–226 and 234–251 nm are assigned to intraligand π–π^* transitions [17], whereas the band at 281–295 nm may be due to charge transfer from coordinated ligand to manganese. The d–d transition bands were not observed in these complexes.

3.2. *Electrochemical and magnetic studies*

Cyclic voltammetry of **2** was performed on acetonitrile solution of samples containing 0.10 M $[N(n\text{-}Bu)_4]PF_6$ as supporting electrolyte. Irreversible reduction potentials at −1.05 and −1.54 V were observed due to a ligand-centered and metal-centered reduction, respectively, as reported earlier [18]. No oxidation response was found.

Variable temperature (5–300 K) molar magnetic susceptibility (χ_M) of binuclear complex **1** is given in figure 1. The magnetic data were analyzed using the Van Vleck equation, based on the magnetic exchange Heisenberg Hamiltonian $H = -2JS_1S_2$ ($S_1 = S_2 = 5/2$). The resulting expression equation (1) was used to fit the experimental data (solid lines in figure 1) with the parameters: $J = -0.17\,\text{cm}^{-1}$, $g = 2.030$.

$$\chi_M T = \frac{Ng^2\mu_B^2\left(2e^{2x} + 10e^{6x} + 28e^{12x} + 60e^{20x} + 110e^{30x}\right)}{k(1 + 3e^{2x} + 5e^{6x} + 7e^{12x} + 9e^{20x} + 11e^{30x})} \tag{1}$$

where $x = J/kT$. At room temperature, $\chi_M T$ shows a value of $8.399\,\text{cm}^3\,\text{K}\,\text{mol}^{-1}$ which is expected for two Mn(II) ions. When the temperature decreases, $\chi_M T$ decreases smoothly until 50 K where it reaches $4.436\,\text{cm}^3\,\text{K}\,\text{mol}^{-1}$ and then more abruptly to $0.143\,\text{cm}^3\,\text{K}\,\text{mol}^{-1}$ at 5 K. The χ_M value increases continuously on cooling from $0.027\,\text{cm}^3\,\text{mol}^{-1}$ to a maximum value of $0.094\,\text{cm}^3\,\text{mol}^{-1}$ at approximately 40 K and

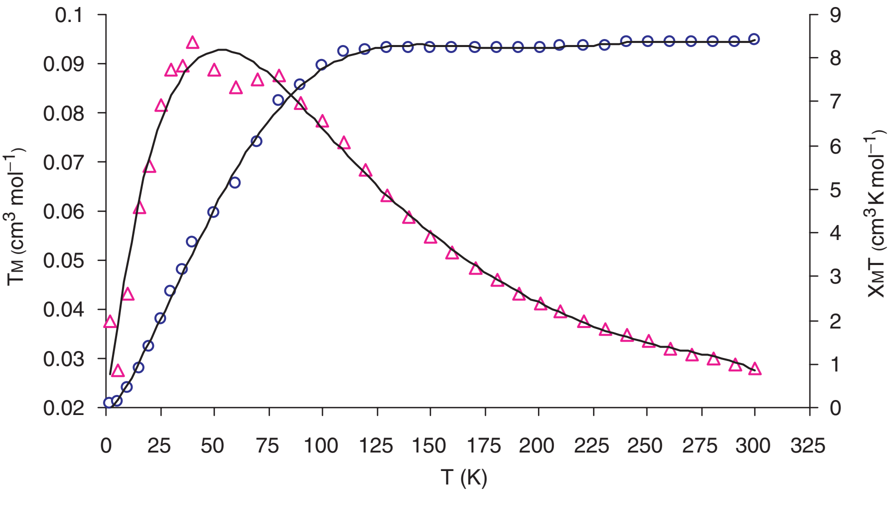

Figure 1. Plot of the $\chi_M T$ product (○) and χ_M (Δ) *vs* T for **1**. The solid line shows the best fit of the data.

then declines rapidly. This indicates an anti-ferromagnetic coupling between two manganese(II) ions which are present at distance of 3.777 Å from each other.

3.3. *Description of crystal structures*

3.3.1. Molecular structure of [$Mn_2(tptz)_2Cl_4$]•CH_3CN (1). Complex **1** crystallizes in triclinic space group *P*-1. The crystallographic data are given in table 1 and important bond lengths and angles are given in table 2. The crystal of **1** contains acetonitrile with high-thermal displacement. Complex **1** (figure 2) is dinuclear with each manganese center six-coordinate with three nitrogens from tptz, two bridging chlorides and one terminal chloride. The manganese–nitrogen bond distances in **1** [Mn(1)–N(1), 2.315(5) Å; Mn(1)–N(2), 2.230(5) Å; Mn(1)–N(3), 2.365(6) Å)] are smaller than reported complexes of the same ligand [18]. The terminal Mn(1)–Cl(1) [2.426(19) Å] is smaller than the bridging Mn(1)–Cl(2) [2.620(2) Å]. The tptz ligand is almost planar; the angles between the central triazine ring and the attached pyridyl rings are 2.6(1), 2.2(1), and 3.6(1)°, which is in accord with the values reported in the literature [19, 20]. Figure 3 shows the formation of a 2-D spiral structure due to the presence of intermolecular C–H $\cdots$ Cl[2.842(14) Å] interaction between CH on pyridine of one complex and

Table 2. Selected bond lengths (Å) and angles (°) for **1**.

Mn(1)–N(2)	2.230(5)	Mn(1)–N(1)	2.315(5)
Mn(1)–N(3)	2.365(6)	Mn(1)–Cl(1)	2.4265(19)
Mn(1)–Cl(2a)	2.4668(19)	Mn(1)–Cl(2)	2.620(2)
N(2)–Mn(1)–N(1)	70.48(18)	N(2)–Mn(1)–N(3)	69.02(18)
N(1)–Mn(1)–N(3)	139.29(18)	N(2)–Mn(1)–Cl(1)	94.96(14)
N(1)–Mn(1)–Cl(1)	100.91(14)	N(3)–Mn(1)–Cl(1)	86.53(14)
N(2)–Mn(1)–Cl(2a)	167.09(14)	N(1)–Mn(1)–Cl(2a)	100.01(14)
N(3)–Mn(1)–Cl(2a)	119.24(14)	Cl(1)–Mn(1)–Cl(2a)	95.46(6)
N(2)–Mn(1)–Cl(2)	86.05(14)	N(1)–Mn(1)–Cl(2)	83.61(14)
N(3)–Mn(1)–Cl(2)	89.71(14)	Cl(1)–Mn(1)–Cl(2)	175.45(7)
Cl(2)–Mn(1)–Cl(2a)	84.16(6)	Mn(1) $\cdots$ Mn(1a)	3.777(27)

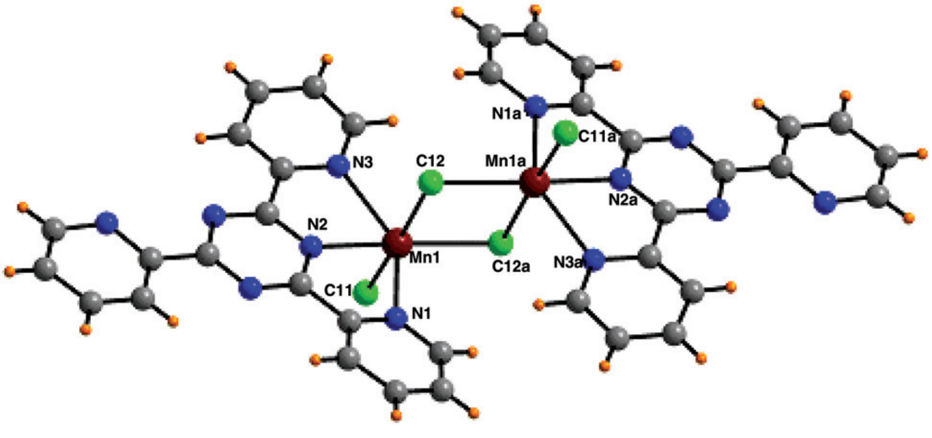

Figure 2. Molecular structure of **1**.

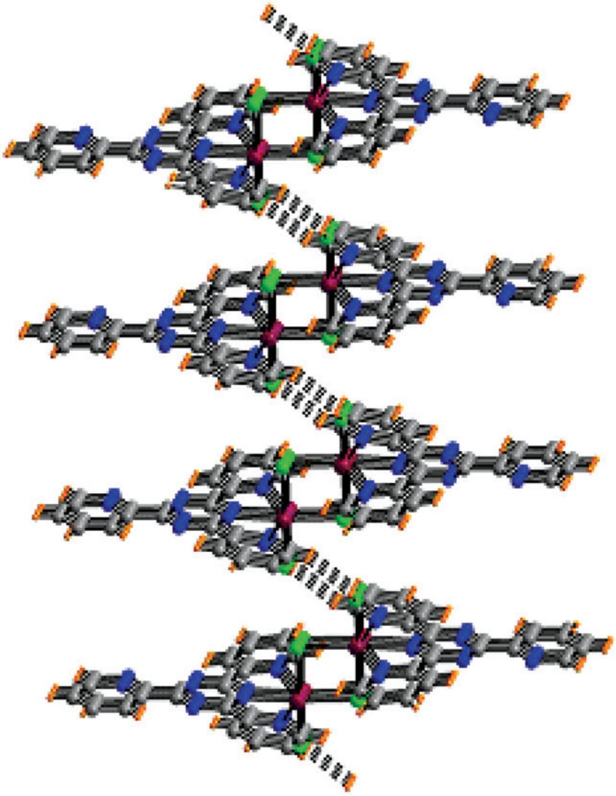

Figure 3. Two-dimensional spiral packing in **1**.

terminal chloride of another complex. The interlayer Mn–Mn separation is 7.421(2) Å along *a*-axis and 9.121(2) Å along the *b*-axis.

3.3.2. Molecular structure of [Mn(tptz)(ac)(N_3)(H_2O)]•H_2O (2). Treatment of **1** with sodium acetate and sodium azide resulted in **2**. The molecular structure of **2** is shown in figure 4. This complex is seven coordinate bonded by three nitrogens from tptz, one nitrogen from azide, two oxygens from acetate, and one oxygen from water. Here, azide is coordinated *trans* to water with Mn(1)–N(7) bond distance of 2.217(14) Å. The Mn–O bond distance [Mn(1)–O(3), 2.198(12) Å] of bound water is shorter than the Mn–O bond distance of coordinated acetate, 2.323(12) and 2.271(12) Å for Mn(1)–O(1) and Mn(1)–O(2), respectively. The Mn–N distance of coordinated azide is also shorter than Mn–N bond distances from tptz (table 3). The bond length between manganese and coordinated oxygen from water as well as nitrogen from azide in the basal plane are shorter than in equatorial sites, 2.271(12)–2.408(12) Å, which are more or less in the range reported in a similar system [19, 21]. Deviation from ideal pentagonal bipyramidal geometry is due to differences in basal angles which vary from 57.19(4)° to 84.47(4)°. The source of distortion primarily comes from bite angle of the ligand. Three types of bond angles are found in the equatorial plane, 57.19(4)° corresponds to the bidentate acetate ligand O(2)–Mn(1)–O(1) bond angle, two intermediate ones of

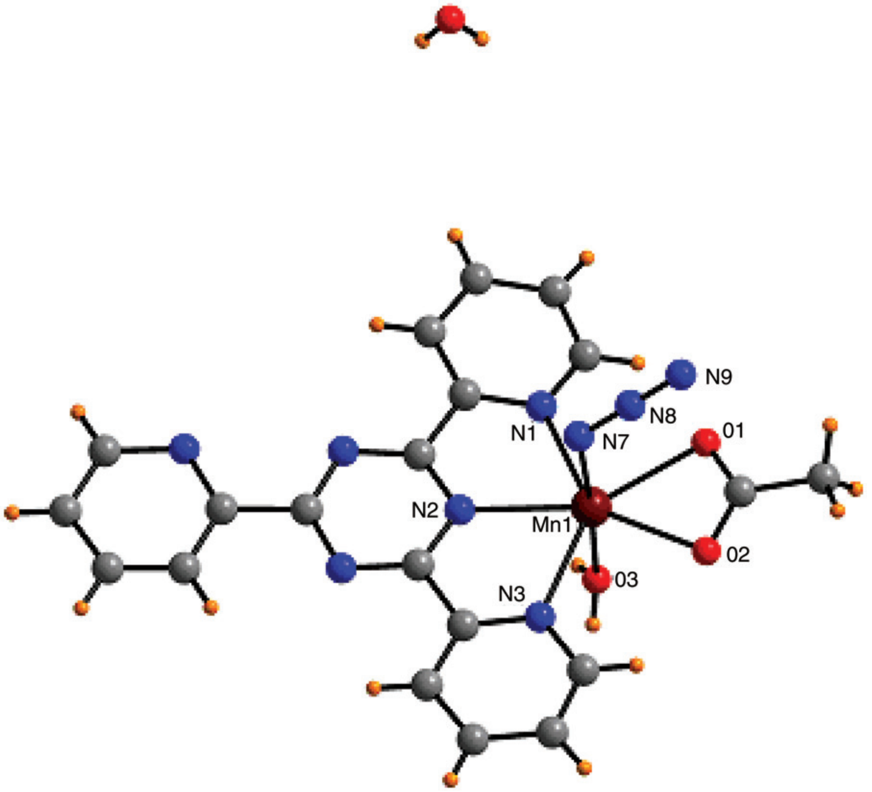

Figure 4. Molecular structure of **2**.

Table 3. Selected bond lengths (Å) and angles (°) for **2**.

Mn(1)–O(3)	2.1983(12)	Mn(1)–N(7)	2.2178(14)
Mn(1)–O(2)	2.2713(12)	Mn(1)–N(2)	2.2921(12)
Mn(1)–O(1)	2.3228(12)	Mn(1)–N(1)	2.3733(13)
Mn(1)–N(3)	2.4076(12)		
O(3)–Mn(1)–N(7)	176.66(5)	O(3)–Mn(1)–O(2)	91.90(5)
N(7)–Mn(1)–O(2)	90.31(5)	O(3)–Mn(1)–N(2)	90.52(5)
N(7)–Mn(1)–N(2)	86.36(5)	O(2)–Mn(1)–N(2)	152.11(4)
O(3)–Mn(1)–O(1)	95.86(5)	N(7)–Mn(1)–O(1)	87.44(5)
O(2)–Mn(1)–O(1)	57.19(4)	N(2)–Mn(1)–O(1)	149.94(4)
O(3)–Mn(1)–N(1)	88.32(4)	N(7)–Mn(1)–N(1)	91.64(5)
O(2)–Mn(1)–N(1)	139.10(4)	O(1)–Mn(1)–N(1)	82.09(4)
O(3)–Mn(1)–N(3)	87.07(4)	N(7)–Mn(1)–N(3)	90.65(5)
O(2)–Mn(1)–N(3)	84.47(4)	N(2)–Mn(1)–N(3)	67.92(4)
O(1)–Mn(1)–N(3)	141.58(4)	N(1)–Mn(1)–N(3)	136.33(4)

67.92(4)° and 68.73(4)° corresponding to the N(tptz)–Mn(1)–N(tptz) bond angles and two greater O(acetate)–Mn(1)–N(tptz) angles of 82.09(4)° and 84.47(4)°. These values are consistent with those found for related complexes [18, 22–26]. The bond distance of Mn(II) to the middle nitrogen N(2) is significantly shorter than Mn(1)–N(1) and Mn(1)–N(3) distances as usually observed in tptz-type ligands [21]. Figure 5 shows

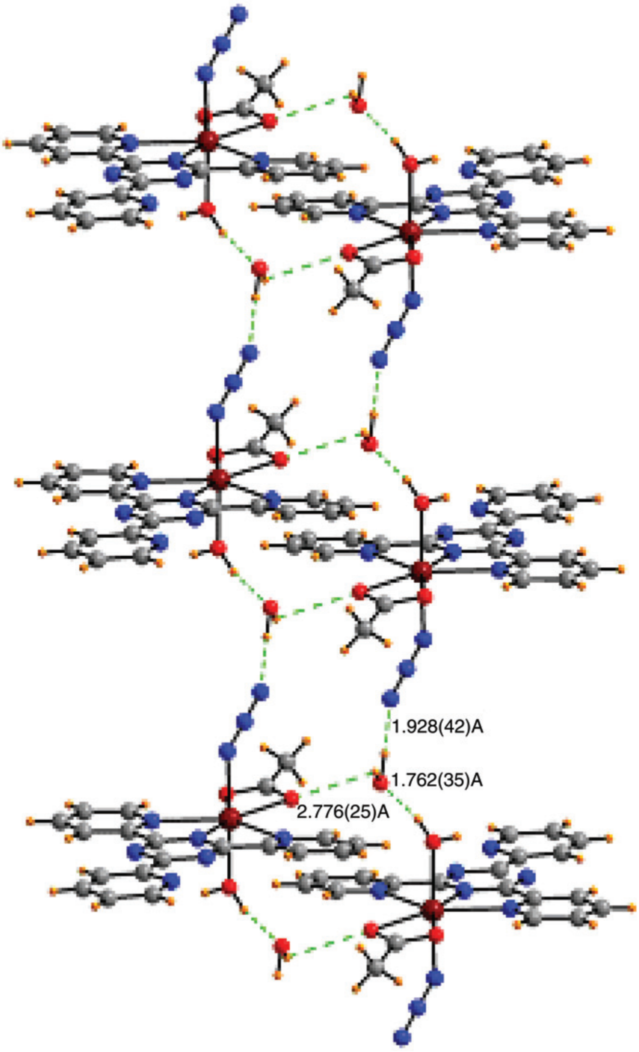

Figure 5. 1-D-layer formed by hydrogen bond interactions in **2**.

different intermolecular interactions in this complex. One uncoordinated water present in the lattice is involved in hydrogen bonding with coordinated water, azide, and acetate, giving a 1-D layered structure. The different intermolecular interactions in this complex resulted in a 3-D network structure (figure 6).

4. Conclusions

We report two complexes of manganese(II). Single crystal X-ray studies demonstrate the presence of different intermolecular interactions resulting in layered structures for **1** and **2**. The azide is terminal in **2** at a distance of 2.218(14) Å. Low-temperature

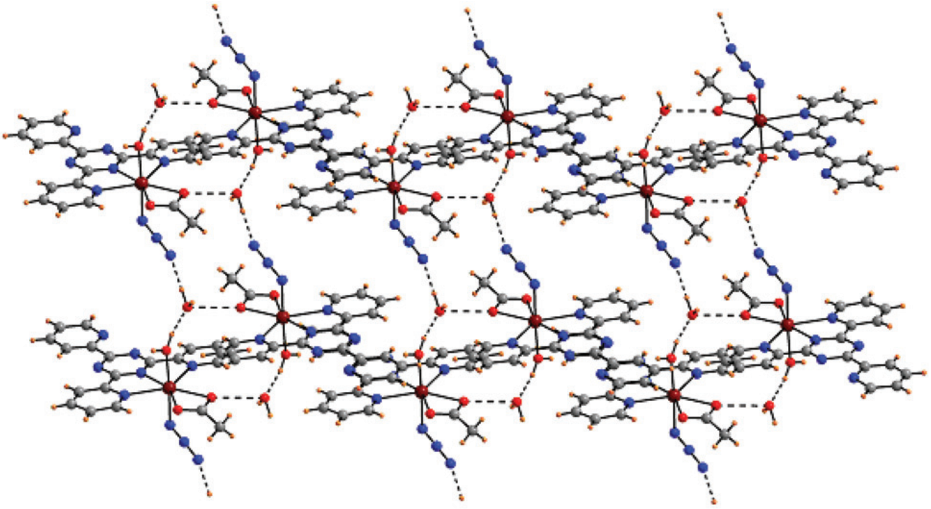

Figure 6. Hydrogen bonds building a 3-D network in **2**.

magnetic measurements for **1** show that this complex has anti-ferromagnetic coupling between Mn centers due to the relatively short separation between them.

Supplementary Material

The crystallographic data have been deposited with CCDC. Supplementary data are available from CCDC, 12 Union Road, Cambridge CB2 1EZ, UK on request by quoting deposition numbers CCDC 675617–675618. Email: deposit@ccdc.cam.ac.uk or www: http://www.ccdc.cam.ac.uk.

Acknowledgments

We are thankful to the DST, New Delhi, for financial support and to Thomas Weyhermüller for magnetic measurement at Max-Planck-Institute für Bioanorganische Chemie, Mülheim, Germany. P. Tyagi is also thankful to CSIR, New Delhi, for providing fellowship in the form of SRF.

References

[1] D. Gatteschi, O. Kahn, J.S. Miller, F. Palacio (Eds). *Molecular Magnetic Materials*, Kluwer Academic Publishers, Dordrecht (1991).
[2] O. Kahn. *Molecular Magnetism*, VCH, New York (1993).
[3] J.S. Miller, M. Drillon (Eds). *Magnetism: Molecules to Materials*, Wiley-VCH, Weinheim (2002).
[4] K. Vrieze, G. van Koten. In *Comprehensive Coordination Chemistry*, G. Wilkinson, R.D. Gillard, J.A. McCleverty (Eds), Vol. 2, p. 225, Pergamon Press, Oxford, England (1987).

[5] (a) K. Dehnicke, J. Strahle. *Angew. Chem., Int. Ed. Engl.*, **31**, 955 (1992); (b) W.A. Nugent, B.L. Haymore. *Coord. Chem. Rev.*, **31**, 123 (1980); (c) J.T. Groves, T. Takahashi. *J. Am. Chem. Soc.*, **105**, 2074 (1983); (d) J.T. Groves, T. Takahashi, W.M. Butler. *Inorg. Chem.*, **22**, 884 (1983); (e) J.D. Bois, J. Hong, E.M. Carreira, M.W. Day. *J. Am. Chem. Soc.*, **118**, 915 (1996).
[6] A. Das, G.M. Rosair, M.S.E. Fallah, J. Ribas, S. Mitra. *Inorg. Chem.*, **45**, 3301 (2006).
[7] E.-Q. Gao, A.-L. Cheng, Y.-X. Xu, M.-Y. He, C.-H. Yan. *Inorg. Chem.*, **44**, 8822 (2005).
[8] K.C. Mondal, M.G.B. Drew, P.S. Mukherjee. *Inorg. Chem.*, **46**, 5625 (2007).
[9] F.-C. Liu, Y.-F. Zeng, J.-P. Zhao, B.-W. Hu, X.-H. Bu, J. Ribas, J. Cano. *Inorg. Chem.*, **46**, 1520 (2007).
[10] L. Zhang, L.-C. Li, D.-Z. Liao, Z.-H. Jiang, S.-P. Yan, P.-W. Shen. *Inorg. Chim. Acta*, **320**, 141 (2001).
[11] N. Liu, A.-L. Cheng, H.-Q. Peng, E.-Q. Gao, M.-Y. He. *Struct. Chem.*, **18**, 43 (2007).
[12] C. Mantel, A.K. Hassan, J. Pecaut, A. Deronzier, M.-N. Collomb, C. Duboc-Toia. *J. Am. Chem. Soc.*, **125**, 12337 (2003).
[13] A.K. Ghosh, D. Ghoshal, J. Ribas, E. Zangrando, N.R. Chaudhuri. *J. Mol. Struct.*, **796**, 195 (2006).
[14] D.D. Perrin, W.L. Armarego, D.R. Perrin. *Purification of Laboratory Chemicals*, 2nd Edn, Pergamon, New York (1980).
[15] G.M. Sheldrick. *Acta Cryst.*, **A46**, 467 (1990).
[16] G.M. Sheldrick. *SHELXTL-NT 2000 Version 6.12, Reference Manual*, University of Göttingen, Göttingen, Germany (2000).
[17] A.B.P. Lever. *Inorganic Electronic Spectroscopy*, 2nd Edn, Elsevier Science, Amsterdam (1984).
[18] A. Majumder, G. Pilet, M.T.G. Rodriguez, S. Mitra. *Polyhedron*, **25**, 2550 (2006).
[19] A. Majumder, C.R. Choudhury, S. Mitra, C. Marschner, J. Baumgartner. *Z. Naturforsch.*, **60b**, 99 (2005).
[20] J. Kim, S. Han. *Acta Crystallogr., Sect. C*, **58**, m521 (2002).
[21] A. Escuer, F.A. Mautner, N. Sanz, R. Vicente. *Inorg. Chim. Acta*, **340**, 163 (2002).
[22] C.W. Chan, C.M. Che, S.M. Peng. *Polyhedron*, **12**, 2169 (1993).
[23] A. Claramunt, A. Escuer, F.A. Mautner, N. Sanz, R. Vicente. *J. Chem. Soc., Dalton Trans.*, 2627 (2000).
[24] M.K. Kabir, M. Kawahara, H. Kumagai, K. Adachi, S. Kawata, T. Ishii, S. Kitagawa. *Polyhedron*, **20**, 1417 (2001).
[25] M.K. Kabir, M. Kawahara, K. Adachi, S. Kawata, T. Ishii, S. Kitagawa. *Mol. Cryst. Liq. Cryst.*, **376**, 65 (2002).
[26] K.K. Cheung, W.T. Wong. *Chem. J. Chin. Univ.*, **21**, 5 (2000).